



1 **Evolution of flood generating processes under climate change in**  
2 **France**

3

4 Yves Trambly <sup>1</sup>, Guillaume Thirel <sup>2,3</sup>, Laurent Strohmer <sup>2,4</sup>, Guillaume Evin <sup>5</sup>, Lola Corre  
5 <sup>6</sup>, Louis Heraut <sup>7</sup>, Eric Sauquet <sup>7</sup>

6

7

8 <sup>1</sup> Espace-Dev, Univ. Montpellier, IRD, Montpellier, France

9

10 <sup>2</sup> University of Paris-Saclay, INRAE, HYCAR, Antony, France

11

12 <sup>3</sup> Univ Toulouse, CNES/IRD/CNRS/INRAE, CESBIO, Toulouse, France

13

14 <sup>4</sup> Department of Ecohydrology and Biogeochemistry, Leibniz Institute of Freshwater Ecology  
15 and Inland Fisheries (IGB), Berlin, Germany

16

17 <sup>5</sup> Univ. Grenoble Alpes, INRAE, CNRS, IRD, Grenoble INP, IGE, Grenoble, France

18

19 <sup>6</sup> CNRM, Université de Toulouse, Météo-France CNRS, Toulouse, France

20

21 <sup>7</sup> INRAE, UR RiverLy, Villeurbanne, France

22

23

24

25 Correspondance to: Yves Trambly ([yves.trambly@ird.fr](mailto:yves.trambly@ird.fr))

26

27

28

29

30

31

32

33

34

35

36

37

38

39

40

41

42

43

44

45

46

47



## 48 **Abstract**

49

50 The impact of climate change on floods varies spatially, and often the observed trends in flood  
51 characteristics can be explained by differentiated changes in flood-generating processes. This  
52 study explores changes in flood magnitude and flood-generating processes under different  
53 climate change scenarios for a large number of basins in France. It is based on an  
54 unprecedented exercise to model the impacts of climate change on hydrology, using a semi-  
55 distributed model (GRSD) applied to 3727 basins with 22 Euro-CORDEX bias-corrected  
56 climate projections using two greenhouse gas emission scenarios (RCP4.5 and RCP8.5).  
57 Annual maxima of daily simulated streamflow were extracted for the period 1975-2100,  
58 resulting in a set of over 10 million flood events, and a trend analysis was carried out on both  
59 flood magnitudes and flood generating processes. The trends in flood magnitude are  
60 contrasted, with increasing trends only in the northern regions of France, although multi-model  
61 convergence rarely exceeds 60 %. The highest increases are observed for the rarest floods  
62 and under the RCP8.5 scenario. A classification of floods according to their generating  
63 process revealed that floods linked to soil saturation represent more than half of all floods in  
64 France. The relative change in the importance of the different flood-generating processes is  
65 not spatially homogeneous and varies by region. The proportion of floods linked to soil  
66 saturation excess is decreasing while the proportion of floods linked to infiltration excess  
67 related to extreme rainfall is increasing, particularly in the southern Mediterranean regions.  
68 Both the frequency and magnitude of floods linked to snowmelt processes are decreasing in  
69 mountainous areas. On the contrary, the most extreme floods associated with rainfall on dry  
70 soils tend to increase, in line with the increase of rainfall intensity. Overall, trends in antecedent  
71 soil moisture conditions are as important as trends in intense rainfall to explain flood hazard  
72 trends in the different climate projections. This study shows how important it is to decipher the  
73 changes in the different flood generating processes in order to better understand their  
74 evolution in different hydroclimatic regions.

75

## 76 **1- Introduction**

77

78 The impact of climate change on floods is uncertain, or unknown, in many regions of the world  
79 (Intergovernmental Panel On Climate Change (IPCC), 2023). In particular, it has been shown  
80 that competing changes in flood-generating processes can modulate, or even offset, changes  
81 in flood hazards (Ivancic and Shaw, 2015; Sharma et al., 2018; Tramblay et al., 2019; Brunner  
82 et al., 2021; Zhang et al., 2022). For example, in the context of an increase in intense rainfall  
83 events in some temperate and arid regions, the concomitant drop in soil moisture, resulting in  
84 lower runoff coefficients, could result in a lack of trend in flood magnitude (Wasko and Nathan,  
85 2019; Ho et al., 2022; Tramblay et al., 2023; Scussolini et al., 2023). Similarly, the large decline  
86 in the frequency of snowmelt-induced floods in many regions may compensate for the  
87 increasing proportion of floods caused by rainstorms, resulting in the absence of trends in  
88 overall flood hazards in numerous regions worldwide where snowmelt is prevalent (Zhang et  
89 al., 2022). To comprehend the evolution of floods, it is essential to analyze not only their  
90 severity but also to consider in detail whether the processes that underpin them are also  
91 changing (Tarasova et al., 2019; Kemter et al., 2020; Blöschl, 2022a, b; Jiang et al., 2022;  
92 Tarasova et al., 2023; Kemter et al., 2023; McMillan et al., 2025). This is particularly salient  
93 given that trends in extreme rainfall do not generally translate into the same trends in floods  
94 (Ivancic and Shaw, 2015; Sharma et al., 2018; Wasko et al., 2023). Numerous studies have  
95 focused on understanding and categorizing floods according to the hydroclimatic mechanisms



behind their generation (Tarasova et al., 2019; Stein et al., 2020; Kemter et al., 2023). We can distinguish studies that use seasonality to categorize the various causal mechanisms based on their temporal proximity (Berghuijs et al., 2016, 2019; Trambly et al., 2021) from other studies that use different hydrological criteria, predominantly thresholds on precipitation intensity, snowmelt, or soil moisture levels, to differentiate between different types of floods (Froidevaux et al., 2015; Tarasova et al., 2018; Kim et al., 2019; Tarasova et al., 2020; Stein et al., 2020, 2021; Trambly et al., 2022; Tarasova et al., 2023; Trambly et al., 2023).

To provide future flood projections, it is necessary to use hydrological models to translate climate projections into hydrological projections, i.e. providing simulated streamflow values for the future. Such a modeling chain, which is generally constituted by greenhouse gas concentration scenarios, global (GCM) and regional (RCM) climate models, bias-correction methods, and hydrological models, necessarily suffers from uncertainties (Clark et al., 2016). The evolution of our society is inherently unpredictable, and thus, climate scenarios describe its evolution through greenhouse gas concentrations (Meinshausen et al., 2020). These concentrations, in turn, influence climate model outputs, which are subject to uncertainties related to process representation and climate variability (Knutti and Sedláček, 2013). Additionally, bias-correction methods and hydrological models are affected by process representation uncertainties (Teutschbein and Seibert, 2012; Maraun et al., 2017). Furthermore, their application in an extrapolation mode may compromise their temporal transferability. Indeed, these models and methods are generally calibrated, optimized, and evaluated over well-known past periods. With climate projections, they are used under potentially very different conditions, with unprecedented air temperatures, and possibly very different precipitation regimes, which may alter their transferability. This issue has been extensively documented in the context of hydrological modeling (Brigode et al., 2013; Thirel et al., 2015b; Dakhlaoui et al., 2017), and various protocols have been proposed to assess the robustness of these models (Klemeš, 1986; Thirel et al., 2015a). It is important to note that models of varying complexity exist, depending on their spatial discretization and the processes included in the equations, as well as the use of automatic parameter optimization (Hrachowitz and Clark, 2017). For large-scale studies, at the regional or even the global scale, most often the hydrological models are not calibrated for all stations but sometimes only in a subset of basins (Alfieri et al., 2015; Roudier et al., 2016; Do et al., 2020; Di Sante et al., 2021; Zhang et al., 2022). Nevertheless, all types of models can suffer from robustness issues (Santos et al., 2025). However, it has been shown that the relative uncertainty associated with hydrological modeling is typically lower for high flows, which are the focus of this study, in comparison to low flows (Vidal et al., 2016; Lemaitre-Basset et al., 2021).

This study analyzes a large ensemble of hydrological projections based on climate projections for a diverse set of basins in France, which represents a range of varied physiographic properties. The aim is to investigate the future evolution of flood events, both in terms of magnitude and flood-generating processes. The methodology enables a multi-factorial analysis of floods and the processes underlying their generation, leading to a better understanding of which factors most influence flood trends. By distinguishing the hydro-climatic drivers regionally, we identify those that may either increase or decrease future flood risks.



## 2- Data and Methods

### 2.1 Hydrological model

The GRSD model, a semi-distributed rainfall-runoff model based on the lumped GR4J model structure (Perrin et al., 2003) and the CemaNeige snow model (Valéry et al., 2014), has been chosen for this study. The rationale behind this choice is its capacity to be applied to a very large range of hydro-meteorological conditions and numerous basins across the world, as shown by the GR4J or GRSD applications in Brazil (Kuana et al., 2024), Nepal (Nepal et al., 2017), Iran (Jahanshahi et al., 2025), Haiti (Bathelemy et al., 2024), Chile (Abbenante et al., 2024), Australia (Stephens et al., 2019), and France (De Lavenne et al., 2019; Lemaitre-Basset et al., 2024), as well as its large number of applications in the context of climate change (Chauveau et al., 2013; Cornelissen et al., 2013; Tian et al., 2013; Fabre et al., 2016; Stephens et al., 2018; Givati et al., 2019; Thirel et al., 2019; Tarek et al., 2021; Wasko et al., 2023; Poncet et al., 2024). The GRSD model calibration and simulation were applied within the airGR and airGRiwrn open-source R packages (Coron et al., 2017; Dorchie, 2022).

GR4J is a four-parameter rainfall-runoff model consisting of two conceptual stores: a production store and a routing store, whose flows are routed to the river after transformation by a unit hydrograph. While the GR4J model is applied on a sub-catchment spatial scale, and the simulated streamflow is routed from upstream to downstream with a lag function (de Lavenne et al., 2019), the CemaNeige snow model uses an additional sub-division of each sub-catchment into five zones of equal area to better describe the process heterogeneities linked to the topography (Valéry et al., 2014). GRSD provides daily streamflow simulation covering 3727 simulation points in France, and different variables have been extracted: the total, solid, and liquid precipitation, the soil water index (SWI, i.e. the ratio between water content and the storage capacity of the production store), and the snowmelt discharge (SMD, i.e. the water flow resulting from snowpack melting). The GRSD model has been calibrated over the 1976-2019 period, using the Kling-Gupta Efficiency criterion (Gupta et al., 2009) applied on squared-root transformed streamflow, against the observed streamflow of 611 gauging stations in France considered as nearly natural (Strohmenger et al., 2023), using the SAFRAN (Vidal et al., 2010) reanalysis as meteorological input. To simulate streamflow over the remaining - ungauged - stations, parameters were transferred from neighbor gauged catchments to the target ungauged catchments following Oudin et al. (2008), and these parameter sets were used to produce pseudo-observed streamflow on the ungauged stations, on which the GRSD model was subsequently calibrated (Sauquet et al., 2024, 2025).

### 2.2 Climate simulations

The GRSD model was thereafter applied using as inputs climate projections from the Explore2-Climat-2022-ADAMONT dataset (Corre et al., 2025), available on the French national climate data portal (*DRIAS - les futurs du climat* - [www.drias-climat.fr](http://www.drias-climat.fr)). This ensemble is derived from the 12-km resolution EURO-CORDEX ensemble (Jacob et al., 2018; Vautard et al., 2021), which consists of regional climate model simulations that downscale global climate model simulations over Europe from the CMIP5 (5th phase of the Coupled Model Intercomparison Project, (Taylor et al., 2012)). For this study, we use the 11 GCM/RCM pairs for which both emission scenarios (RCP4.5 and RCP8.5) are available (Table T1 in supplementary materials). The outputs of the climate models were statistically adjusted over



mainland France, against the 8- km resolution SAFRAN reanalysis (Vidal et al. 2010). The bias correction method consists of a quantile mapping relying on seasonal weather regimes (ADAMONT method, Verfaillie et al., 2017). In the following, we use the daily rainfall data and the variables used to compute evapotranspiration (temperature, relative humidity, wind, radiation) from these bias adjusted simulations. These data are available from 1975-2100 at the daily time scale with an 8-km spatial resolution and have been aggregated at the catchment scale.

Several studies describe the future climate changes in France based on these projections (Marson et al., 2024). Overall, they show a shift towards hotter and drier summers, as well as an expansion of temperate climate in mountainous regions (Strohmenger et al., 2024). Despite variations in the magnitude of warming depending on the scenario, time horizon, or level of warming considered, all studies identify common features. These include spatial contrasts, with stronger warming projected in the south, east, and mountainous regions compared to the Atlantic coast, showing a gradient of about 1°C. Seasonal contrasts are also consistent, with warming more pronounced in summer than in winter (with also a difference of 1°C). Regarding precipitation, all studies highlight the limited agreement among models on the annual average, which is linked to the influence of internal variability and to France's geographical position, which places it in a transition zone between Northern Europe, where precipitation is projected to increase, and the Mediterranean region, where it is projected to decrease (Terray and Boé, 2013; Coppola et al., 2021). On a seasonal scale, however, projections are more consistent. In winter, median changes show an increase in rainfall (particularly in the northern regions) alongside a notable decrease in snowfall, especially in the low- and mid-mountain ranges. In summer, projections indicate a decrease in rainfall (particularly in the southern half). These changes in precipitation combined with increased evaporation due to warming, lead to a decrease in water resources availability and, consequently, a marked drying of the soil. In terms of intense rainfall (characterized by the annual maximum daily rainfall), the climate models show large dispersion regarding the direction of future changes (Tramblay et al., 2024), except for the long-term horizon under the RCP8.5 scenario or for high levels of warming (e.g., +4°C on average across France), where they tend to agree on an increase, particularly in the northern part of France

### 2.3 Extraction of flood events

From this dataset, we focused on the annual maximum of daily streamflow that has been extracted for each simulation point. For each station, a time series of 124 values, between 1976 and 2099 considering hydrological years starting in September, is available and described thereafter as the Annual Maximum Flood (AMF) series, referred to as 'floods' to improve readability. This sampling results in a total of 10,167,256 flood events. To estimate the base flow contribution, that is the proportion of direct runoff from rainfall and/or snowmelt, we applied a base flow filter (Lyne and Hollick, 1979) to compute the direct streamflow fraction. To extract the characteristics of the events in terms of rainfall and snowmelt, we computed the antecedent cumulative rainfall and snowmelt for each AMF value, and this aggregation stops if a day has rainfall below 1 mm or if a maximum of seven days is reached. Thus, this duration estimated for each event is extracted and hereafter referred to as the time of concentration, which may differ for each event. This time window of seven days is chosen given the size of the basins considered in the present study (from 64 to 111 570 km<sup>2</sup>) and also to be consistent with previous studies using similar approaches (Ivancic and Shaw, 2015; Stein et al., 2020).



For each simulated flood event, we extracted: the antecedent soil moisture (i.e. SWI, between zero and one) one day before the flood date, the concentration time (in days), the total and maximum daily rainfall (mm) during the event, the fraction of the total flood streamflow being direct streamflow (%), and the total snowmelt discharge (mm) during the event.

## 2.4 Classification of flood events

The flood event classification was determined using a decision tree that had previously been applied in Europe and the USA (Kemter et al., 2020, 2023) to estimate the importance of five different flood-generating processes in each catchment, namely long rain, short rain, snowmelt, rain and snowmelt, and soil moisture excess. This classification is based on the catchment and climatic conditions occurring during the period defined by the time of concentration before the day of the flood peak. The rationale behind the choice of this classification over others (e.g. Tarasova et al., 2019) is that it does not rely on fixed quantities for the different variables, and notably precipitation extremes, compared to other classification schemes (Stein et al., 2020; Trambly et al., 2022, 2023). Indeed, in a climate change context, these quantities could vary over time, notably those related to extreme rainfall that are inherently difficult to estimate precisely using climate simulations at these spatial and temporal resolutions (8 km, daily).

The flood event classification from Kemter et al. (2023) is adapted using the following sequential rules:

1. If the snowmelt is larger than the rainfall, the event is classified as 'snowmelt',
2. If the snowmelt is larger than 25 % of the rainfall, the event is classified as 'rain and snowmelt',
3. If antecedent soil moisture before the event is larger than the soil moisture threshold, the event is classified as 'soil water excess',
4. If during the event, the daily maximum rainfall exceeds 75 % of the total rainfall, the event is classified as 'short rain',
5. Else, the event is classified as 'long rain'.

In the present study, we estimated the soil moisture threshold for each basin to identify flood events related to soil moisture excess. Considering specific soil moisture thresholds for each basin is undoubtedly more realistic than using a single soil saturation threshold for all basins, as done in other studies. The approach used herein has been applied previously (Tarasova et al., 2018; Trambly et al., 2022) and is data-based, since there is no method for estimating these thresholds a priori from catchment characteristics. It relies on the extraction of all streamflow events above the 10th percentile of the whole streamflow time series between 1975 and 2005, fitting an exponential function to the soil moisture/runoff relationship, and then to identify the inflection point in the soil moisture/runoff relationship (i.e., the max slope of the curve). Here, we apply the Pruned Exact Linear Time method (Killick et al., 2012) to detect a change point (i.e., the soil moisture threshold, figure S1) in the exponential fit.





## 288 **2.5 Trend detection**

289

290 To check for trends, the entire annual time series between 1976 and 2099 was considered.  
291 The rationale for using trend detection over the whole record is that floods in many regions  
292 are strongly impacted by multidecadal variability, notably in Europe (Hodgkins et al., 2017;  
293 Lun et al., 2020; Blöschl et al., 2020), making it difficult to detect climate change response  
294 using the standard approach of comparing historical and future time windows of about 30  
295 years. Two approaches are applied to detect these trends. First, a quantile regression  
296 (Koenker and Bassett, 1978), is applied to check the presence of trends in the 2-year flood  
297 and in the 20-year flood. The significance of these trends at the 5 % level is then assessed  
298 using a bootstrap method (Efron, 1979). In this case, the magnitude of the trend is given by  
299 the slope of the regression. We also applied a variant of the Mann-Kendall test adjusted for  
300 serial correlation in the data (Hamed and Ramachandra Rao, 1998), and the Sen slope (Sen,  
301 1968) method to estimate the magnitude of the trends. The Mann-Kendall test was applied to  
302 the different flood event characteristics, as well as the relative frequencies of the different flood  
303 event types. In that latter case, 20-year sliding windows were used to compute these  
304 frequencies, using a similar approach as in Tarasova et al. (2023). Given that some processes  
305 are not relevant to all basins (e.g. snowmelt), we applied the trend detection test only if a  
306 minimum of 20 occurrences for the given flood process is present in the data sample over the  
307 1975-2100 period. To present the trend detection results, we considered the multi-model index  
308 of agreement (MIA) (Tramblay and Somot, 2018) that describes the model convergence  
309 towards an increase (1) or a decrease (-1) for a given indicator. The objective is to identify  
310 robust changes, where all model projections converge towards the same result.

311

## 312 **3- Results and discussion**

313

### 314 **3.1 Changes in flood characteristics**

315

316 Flood trends are analyzed here using the quantile regression technique, which distinguishes  
317 the change signal for AMF corresponding to 2-year (Q50) and 20-year (Q95) return periods.  
318 The results presented in Figure 1 show the convergence of the different simulations under the  
319 RCP4.5 and RCP8.5 scenarios with the MIA index. The figure shows a contrasting signal, with  
320 a relatively good convergence of the models towards an increase in Q50 and Q95 in the  
321 northern half of France and an absence of consensus for trends or even a decrease in some  
322 areas for the southern regions, that is more marked under RCP8.5. Overall, convergence at  
323 the country level is rather weak, with the median MIA value around 0.5 (Figure S2).  
324 Convergence between models is slightly greater for Q50 rather than Q95, expressing a larger  
325 uncertainty for rarest floods. In terms of magnitude (Figure 2), trends are more marked for the  
326 rarest floods (median change +28 % with RCP4.5, +34 % with RCP8.5), than for the most  
327 frequent floods (median change +20 % with RCP4.5, +27 % with RCP8.5). Overall, the  
328 projected changes between Q50 and Q95 are more correlated under the RCP8.5 than under  
329 the RCP4.5. This north/south contrast in the projections is consistent with previous findings  
330 using observational data (Blöschl et al., 2019; Tramblay et al., 2019).

331

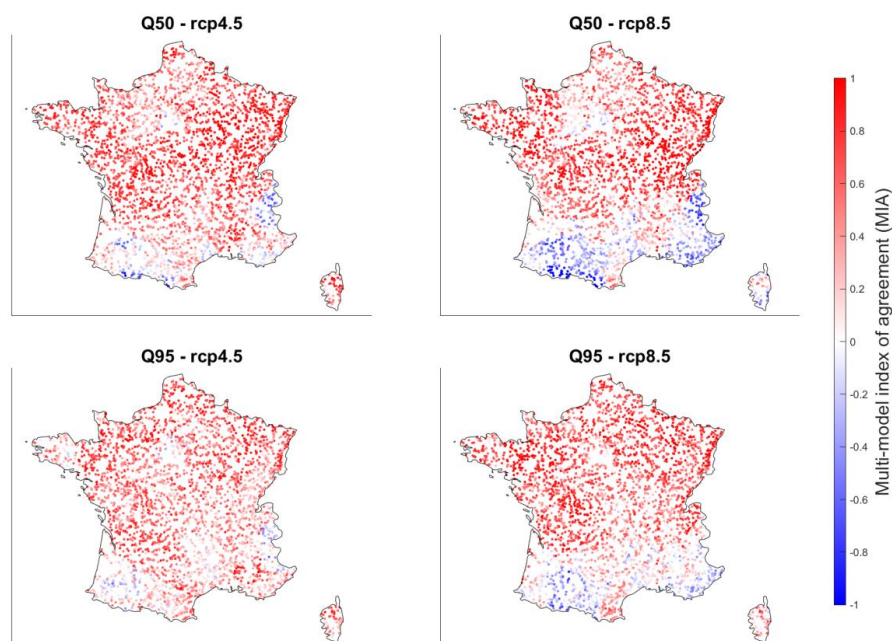


Figure 1: Maps of the multi-model index of agreement for the Q50 (2-year flood) and Q95 (20-year flood) for the 3727 simulation points, for the RCP4.5 and RCP8.5.

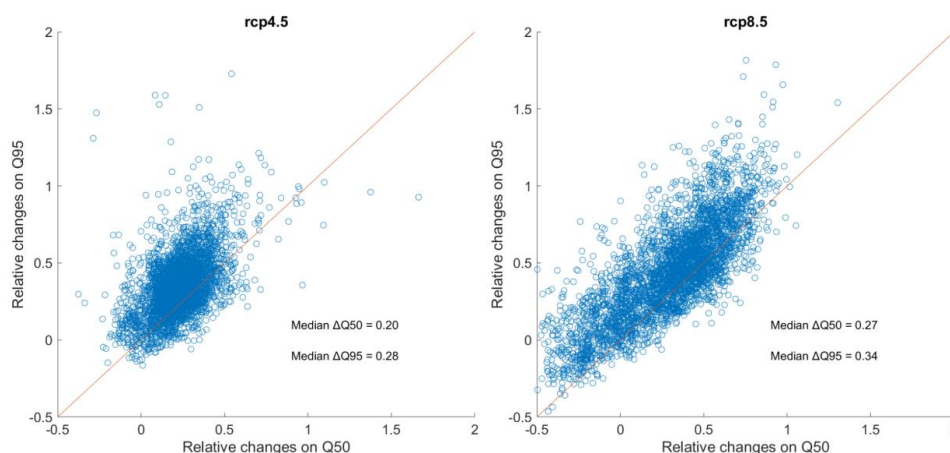


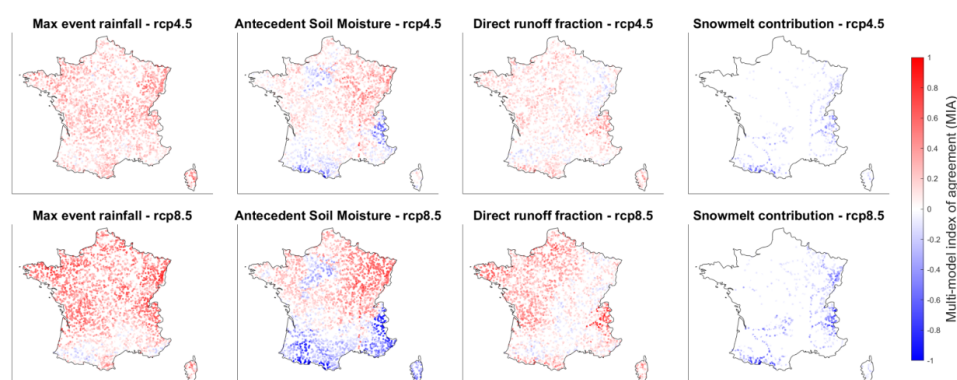
Figure 2: Comparison of the mean multi-model magnitude of significant trends on 2-year (Q50) and 20-year (Q95) floods under the RCP4.5 and RCP8.5.

This analysis of flood trends is complemented by trends in various indicators calculated during floods: maximum daily rainfall during the episode, initial soil moisture conditions, fraction of flood discharge from direct runoff, and contribution of snowmelt to flooding. The trends are shown for the RCP4.5 and RCP8.5 scenarios in Figure 3, with a general increase in maximum





daily rainfall during floods, though less marked in southern France. The trends in antecedent soil moisture are more contrasted, with a good convergence of models towards an increase, more marked for RCP8.5, in the northern half of France and particularly in the eastern region. On the opposite, antecedent soil moisture decreases in the mountainous regions of the Alps and Pyrenees, and around the Mediterranean Sea. For the fraction of direct runoff, there is a slight trend towards an increase in RCP4.5, and a noticeable trend towards an increase in RCP8.5, in the western regions. Finally, the contribution of snowmelt to flood flows is decreasing wherever this component influences floods. Thus, it is interesting to note that in a context of increasing rainfall intensity, outside Mediterranean regions, we observe an increase in flood magnitude, that is associated either with an increase in initial soil saturation conditions, in eastern France, or with an increase in the fraction of direct runoff, in western France. It is also worth noticing that the spatial pattern of soil moisture trends seems to mimic flood trends more closely than extreme rainfall trends, as observed in other regions of the world (Wasko and Nathan, 2019).



362  
363

364 Figure 3: Multi-model index of agreement of the trends in maximum rainfall during floods,  
365 antecedent soil moisture conditions, direct streamflow fraction, and snowmelt fraction, under  
366 the RCP4.5 and RCP8.5 with ADAMONT

367

### 368 3.2 Classification of flood-generating processes

369

370 The floods extracted from the various simulations were classified according to the different  
371 categories; snowmelt, rain and snowmelt, soil water excess, short rain, and long rain. The  
372 result of this classification from the multimodel ensemble during the historical period 1975-  
373 2005 is presented in Figure 4, which shows the relative contribution of these different flood  
374 types for each station. Events linked to soil saturation are predominant, accounting for more  
375 than 50 % of floods in France. Long precipitation events are responsible for almost 25 % of  
376 floods and are mainly located in the north-west and south of France. It should be noted that  
377 most of these events also correspond to soil saturation processes, although in this case, the  
378 soil saturation occurs not before but during these events. Indeed, Figure S3 shows that during  
379 these long rain events, the largest floods are only associated with SWI values above 0.6, and  
380 that the modal value of SWI maxima is close to 0.75 and 0.8, corresponding to the value of  
381 the soil saturation threshold most frequently found in French basins (Figure S1). Snowmelt-



related events, caused by snowmelt or a mixture of rain and snowmelt, account for around 11 % of the total number of floods, mainly for mountainous areas and central-eastern regions. Lastly, short rain events account for less than 10 % of the events, with a spatial distribution very similar to that of long rain. In terms of magnitude, when all the standardized floods for the different processes are grouped, short rain events show the highest magnitude, followed by soil water excess and long rain events, which have similar magnitudes (Figure 5a).

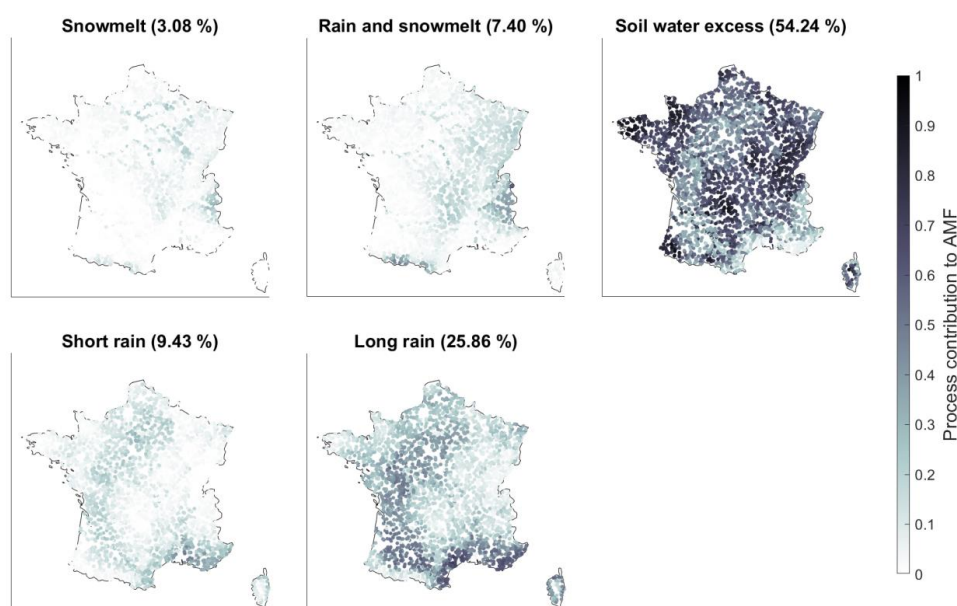
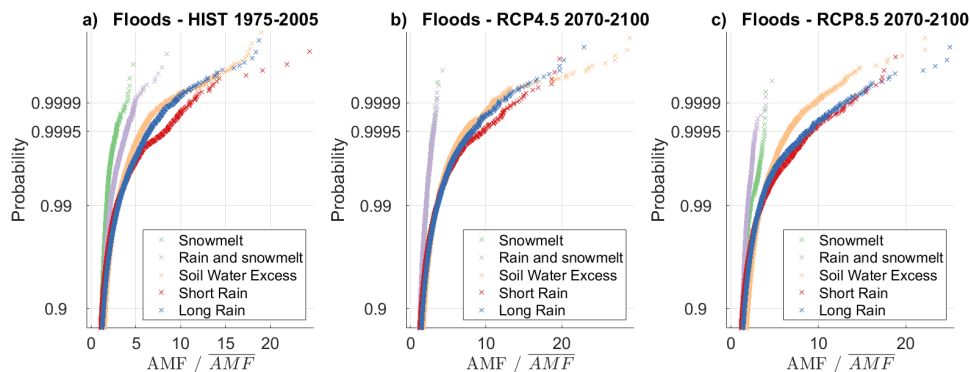


Figure 4: Relative proportion of the different flood-generating processes for each basin during the historical period 1975-2005. The average contribution of each process to the total number of floods is given in the titles of the sub-plots in percentages.

As these results are obtained with an ensemble of bias-corrected climate projections, the results have also been extracted for each GCM/RCM couple independently to check the consistency between results. Over the historical period, the classifications obtained with the different climate models show a very high degree of consistency in the proportions of the different classes between models (Figure S4). This result was quite expected given that the RCM simulations are bias-corrected using the same reference. The results of this classification are also very consistent with previous studies in Europe applying similar classification schemes but with different datasets and a different methodology. For instance, Berghuijs et al. (2019) have found that 49 % of floods are driven by soil water excess in Western Europe, and about 22 % of floods are driven by maximum annual rainfall. Tarasova et al. (2023) obtained similar results in their pan-European study using slightly different classes, with 11 % of rain on dry soils, 67 % of rain on wet soils, and 21 % of rain-on-snow events in Atlantic regions, and for the Mediterranean region, with 25 % of rain on dry soils, 59 % of rain on wet soils, and 15 % of rain-on-snow events. In both regions, the proportion of snowmelt-only driven floods was equivalent to 1 % only.



410  
411



412  
413

414 Figure 5: Distribution of floods all basins together, for the different types of floods during the  
415 historical period 1975-2005, and for 2070-2100 under RCP4.5 and RCP8.5

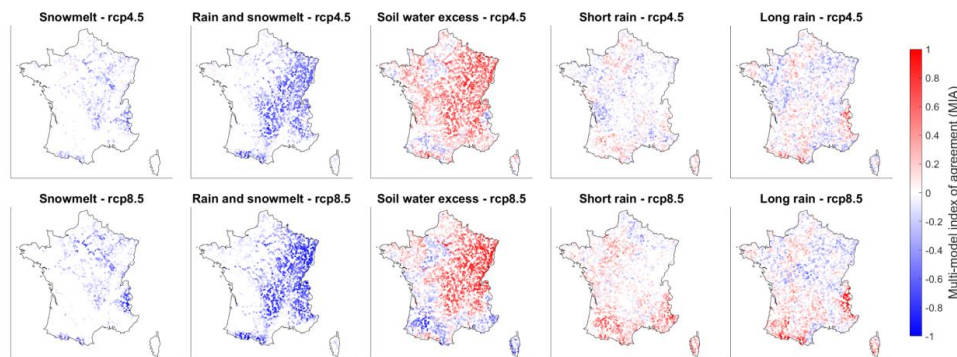
416  
417

### 418 3.3 Changes in flood-generating processes

419

420 The direction of changes in the contribution of the various flood-generating processes in  
421 RCP4.5 and RCP8.5 is shown in Figure 6. Given the low frequency of snowmelt-only events,  
422 it is difficult to draw robust conclusions about changes in these events. However, there is a  
423 general decrease in snowmelt or rain-and-snowmelt-induced floods in both scenarios. This  
424 applies both to the mountain ranges of the Alps and the Pyrenees and to regions located from  
425 the center of France to the northeast. There is also an increase in the contribution of events  
426 linked to soil saturation, especially in the northeast, that is more widespread spatially for  
427 RCP4.5 than for RCP8.5. Floods induced by short rains and long rains are increasing in areas  
428 where soil water excess events are decreasing, most importantly in the southern regions and  
429 the Alps. It should be noted that the change in rain and snowmelt events shows a very similar  
430 spatial distribution compared to the trends for events linked to soil water excess. Indeed, the  
431 spatial correlations between changes in soil water excess events on the one hand, and rain  
432 and snowmelt events on the other hand, are significant (-0.6 for RCP4.5 and -0.67 for  
433 RCP8.5). This means that where the proportion of events linked to the combination of rain and  
434 snowmelt is reducing, these events tend to be replaced by floods associated with saturated  
435 soils. Similarly, there are significant correlations between changes in the proportion of soil  
436 water excess events and the proportion of short rain or long rain events (correlations of -0.31  
437 between changes in soil water excess and changes in short rain, -0.4 with changes in long  
438 rain under RCP4.5, and respectively -0.54 and -0.45 under RCP8.5 - yet the magnitude of  
439 these correlations remains small). We can therefore see that in regions where the proportion  
440 of floods related to saturated soils is decreasing, the proportion of floods associated with short  
441 rain or long rain is increasing, particularly in southern regions. This result shows that these  
442 shifts, previously observed in historical records (Jiang et al., 2022; Tarasova et al., 2023;  
443 Trambly et al., 2023), are likely to amplify under the two emission scenarios considered  
444 herein.

445  
446



447  
448  
449  
450  
451  
452  
453  
454  
455  
456  
457  
458  
459  
460  
461  
462  
463  
464  
465  
466  
467  
468  
469  
470  
471  
472  
473  
474

Figure 6: Multi-model index of agreement for the trends in the contributions of the different flood-generating processes, under the RCP4.5 and RCP8.5

The trends in the flood quantiles (Q50 and Q95) and the trends in the five flood-generating processes have been clustered for the two RCP separately, using the Ward linkage method, commonly used in hierarchical clustering, together with silhouette plots to identify the optimal number of clusters (Kaufman and Rousseeuw, 1990). This classification results in four spatial clusters as shown in Figure 7. Cluster 1 includes mountain basins in the Alps and Pyrenees, where Q50 and Q95 show mostly declining trends, or an absence of trends, linked to a sharp decrease in snowmelt-related events and an increase in events caused by short rain and long rain. Cluster 2 includes basins located in southern regions, where there is no trend or a decrease in floods, associated with a drop in events linked to soil saturation and an increase in events caused by short rain and long rain. Cluster 3 and 4 gather the stations in the northern half of France, where flooding trends are on the rise, but with a sharp decrease in snowmelt-related flooding in the east (cluster 4), while in the west (cluster 3) there is an increase of the proportion of intense rainfall (short rain) on dry soils, associated with an increase in direct runoff, as already shown in the previous sections. The spatial organization of the different clusters is very similar under the two scenarios RCP4.5 and RCP8.5, with one notable difference concerning cluster 2, corresponding to Mediterranean events in the South of France, which has a much more marked northward extension under the RCP8.5 scenario. Overall, it should be noted that this spatial distribution is strongly reminiscent of the different climatic zones observed in France (Strohmenger et al., 2024), with the western and coastal regions under a temperate oceanic climate, the center and east of France with a more continental climate, the southern part corresponding to areas with a Mediterranean climate, and finally the mountain regions of the Alps and the Pyrenees.

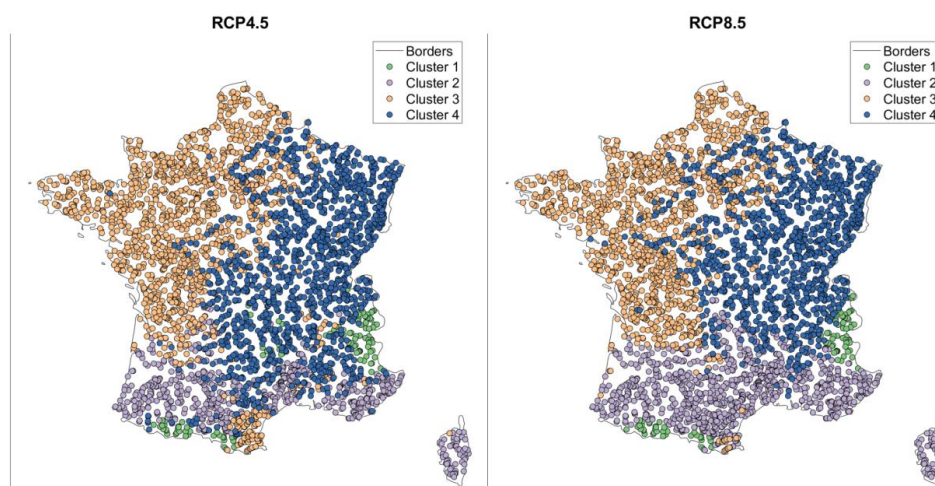


Figure 7: Regional clusters of the trends in flood magnitudes and flood-generating processes

### 3.4 Regional drivers of change for flood hazard in future projections

The magnitude of floods will change differently, depending on their generating processes. When aggregated over France, the magnitude of snowmelt-related events is projected to decrease (Figures 5b and 5c), while soil water excess events increase slightly. It is mainly the magnitude of the rarest and most intense short rain and long rain events that are increasing. Marked differences between future and historical distributions are mainly projected for events associated with non-exceedance probabilities greater than 0.95 (i.e. floods corresponding to a 20-year return period and beyond). However, this overall assessment at the country level hides regional differences depending on the flood-generating processes. If we look by region and by flood process (supplementary figures S5 and S6), we observe that this increase in the magnitude of the rarest floods (i.e. the distribution tails), only affects the northern regions of France, clusters 3 and 4, and events linked to short rains and long rains, which are flood events linked to rainfall on dry soils, and also the events related to soil water excess. Under the RCP4.5, the flood distributions in the different regions for the different flood generating process are similar between 1975-2005 and 2070-2100 (figure S5), except for some of the most extreme events as mentioned above. For the RCP8.5, there are more marked changes, notably with a shift of the flood distribution towards lower values for the cluster 1 (mountainous regions), and to a lesser extent for the cluster 2 (Mediterranean regions). On the opposite, there are distribution shifts towards increased flood magnitudes for most processes in the clusters 3 and 4.

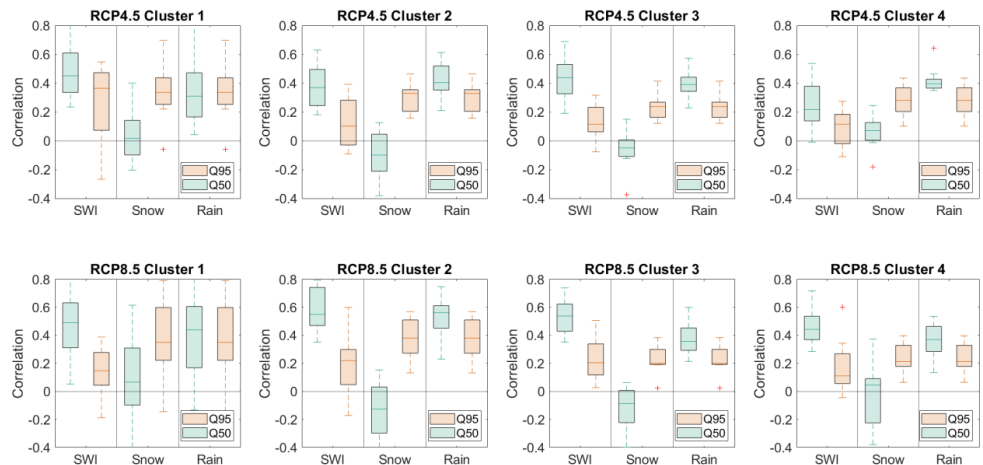
Another important question that arises when analyzing the impact of climate change on floods is to understand which factors have the greatest influence on flood trends in different climate projections. Given that 11 climate projections are available here for RCP4.5 and RCP8.5, we can calculate for each model the correlations between flood trends and the trends in the three factors most commonly recognized as flood triggers (Wasko and Nathan, 2019, Zhang et al., 2022) at the event scale (antecedent soil moisture conditions, snowmelt contribution, and maximal rainfall) and the trends for floods with 2-year (Q50) and 20-year (Q95) return periods.





The results of this correlation analysis are presented in Figure 8 for each of the four regions identified by the clustering of Figure 7. For the first cluster, i.e. the mountain areas, there are strong positive correlations between snowmelt trends and Q95 flood trends, but much more contrasting correlations with Q50. For clusters 2 to 4, the patterns are quite similar. A striking result is that the correlations between trends in floods and trends in SWI are at least equivalent, if not superior, to the correlations with trends in intense rainfall for the different climate projections. This result is not region-specific, and it should also be noted that correlations with SWI are almost systematically stronger for frequent floods (2-year), than for rarer floods (20-year). To a lesser extent, correlations are also weaker between trends in rainfall intensity and the flood trends for the rarest floods, than for trends in the most frequent floods. This result should however be interpreted with caution given the uncertainties inherent in estimating intense rainfall in climate models. These results imply that the trends projected for the various processes can, to a large extent, explain the trends in flooding in France, and that the evolution of soil saturation plays a role equivalent to that of the evolution of intense rainfall in the various regions to explain the trends in flood hazard in the different climate projections.

523  
524



525  
526

Figure 8: Correlations between the trends in event antecedent soil moisture (SWI), snowmelt contribution (Snow) and maximum rainfall (Rain), and the trends in 2-year (Q50) and 20-year (Q95) floods. The boxplots represent the ranges of the correlation coefficients obtained for each climate projection under the RCP4.5 (top row) and RCP8.5 (bottom row).

531  
532  
533  
534  
535  
536  
537  
538  
539  
540





#### 541 **4. Conclusions**

542  
543 Flood trends show a contrasting signal in the different regions, with a fairly good consistency  
544 towards an increase in floods in northern France and an absence of signal in southern regions.  
545 In line with the uncertainty in future precipitation changes, it should be emphasized that multi-  
546 model agreement remains fairly weak in most basins for increasing or decreasing trends in  
547 flood hazard. In terms of magnitude, trends are more marked for rare floods (20-year return  
548 period) than for frequent floods (2-year return period). Trends in initial moisture conditions  
549 show a spatial distribution quite similar to that of floods, with an increase mainly in northern  
550 regions and a decrease in antecedent soil moisture in the south. These changes tend to mimic  
551 the seasonal precipitation changes, with an increase in winter precipitation in the north and a  
552 decrease in summer precipitation in the south. The magnitude of rainfall events increases  
553 everywhere, most markedly in the northern half of France, while the contribution of snowmelt  
554 decreases everywhere in the mountain ranges, consistently with the projected decrease in  
555 snowfall as indicated by climate projections. A classification of floods by process reveals that  
556 floods linked to soil saturation account for more than half of all floods in France, and that this  
557 proportion is increasing in the north-east of the country while decreasing in the south. The  
558 relative changes in the importance of the different flood generating processes is not spatially  
559 homogeneous and varies by region. The analysis highlights that flooding trends can be  
560 decomposed into several distinct signals linked to different flooding processes, and that the  
561 multi-model uncertainty concerning these trends varies according to the process considered.  
562 Trends in soil saturation play as important a role as trends in intense rainfall in different regions  
563 to explain changes in flood hazard in the different climate simulations.

564 Overall, in regions where the proportion of floods linked to saturated soils is decreasing, the  
565 proportion of floods linked to short or long rains is increasing, particularly in the south. Both  
566 the frequency and magnitude of floods linked to snowmelt processes are declining in areas  
567 where these processes operate, namely mountainous areas and the north-eastern regions.  
568 On the contrary, the flood magnitudes associated with rainfall on dry soils (short rain and long  
569 rain floods) tend to increase, in line with the increase of maximum event rainfall in the different  
570 scenarios. The trends in the RCP8.5 scenario are both more pronounced and allow better  
571 discrimination between regions. The changes seem fairly consistent with the distribution of  
572 French climatic zones: floods tend to increase in the continental climate zone, with an increase  
573 in soil water content leading to an increase in the number of flood events linked to soil  
574 saturation. In the temperate oceanic zone, flooding is also on the rise, but this time in  
575 connection with the increased intensity of intense rainfall. In the Mediterranean regions, there  
576 is no marked trend in flooding, with declining soil moisture and uncertain trends in rainfall  
577 intensity. Lastly, in mountainous regions, there are drastic changes in flood-generating  
578 conditions, with a marked drop in snowmelt and an absence of trends, or even a decline, in  
579 flooding.

580 In terms of perspectives for this study, there are a number of points to note. The first is that  
581 the analysis carried out here is based on a daily time step, which is unsuitable for the analysis  
582 of flash floods, which occur, for example, in Mediterranean regions with high hourly rainfall  
583 intensities. For small basins, where only until recently high-resolution convection-permitting  
584 models (Lucas-Picher et al., 2021) are able to tackle this problem by improving the modeling  
585 of small-scale convective rainfall events (Kay, 2022; Poncet et al., 2024), there is not yet a  
586 large ensemble of model runs available to assess the uncertainties in the projections. It should



587 be stressed out that the results obtained herein are unlikely to be transposable to flash floods,  
588 and large convection-permitting model ensembles would be required to replicate such an  
589 analysis for flash floods. Another important aspect is that this study is based on natural  
590 hydrology processes in relation to climate change. However, changes in land use (Roger et  
591 al., 2017; Yang et al., 2021) or the construction of infrastructures, such as dams (Zahar et al.,  
592 2008; Grill et al., 2019; Blöschl, 2022b), can greatly modulate the risk of flooding. However,  
593 this type of non-climate-related change is very difficult, if not impossible, to take into account  
594 in such a large scale and multi-basin study. Nevertheless, at more local scales, and in close  
595 interaction with land-use planning and water management stakeholders, such multi-criteria  
596 analyses could be carried out to better distinguish between climatic and non-climatic  
597 influences on the evolution of flood risk.

598  
599  
600  
601  
602  
603  
604  
605  
606  
607  
608  
609  
610  
611  
612  
613  
614  
615  
616  
617  
618  
619  
620  
621  
622  
623  
624  
625  
626  
627  
628  
629  
630  
631  
632  
633  
634



635 **Data availability**

636

637 All the data of this study is available freely in open access. The bias-corrected climate model  
638 simulations are available at: <https://www.drias-climat.fr/>. The hydrological model simulations  
639 are available at: <https://www.drias-eau.fr/>. The discharge measurements over France are  
640 available at: <https://www.hydro.eaufrance.fr/>. The SAFRAN database is available at:  
641 <https://meteo.data.gouv.fr/datasets/donnees-changement-climatique-sim-quotidienne/>

642

643 All the technical reports of the Explore2 project are available in the repository:  
644 <https://entrepot.recherche.data.gouv.fr/dataverse/explore2>

645

646 **Code availability**

647

648 The bias-correction method for climate simulations is available at:  
649 <https://github.com/yrobink/SBCK-python>

650

651 The hydrological model codes are available at: <https://inrae.github.io/airGRiwrn/> and  
652 <https://hydrogr.github.io/airGR/>

653

654 **Author contributions**

655

656 YT designed the study and performed the experiments. GT, LS, ran the GRSD model  
657 simulations, LH managed the database, LC generated the climate scenarios, GE and ES  
658 contributed to the methodology and YT wrote the paper with contributions from all the  
659 authors.

660

661 **Competing interest declaration**

662

663 The authors declare that they have no conflict of interest.

664

665 **Acknowledgements**

666

667 This research was financed by the Explore2 project with support from the French  
668 Biodiversity Agency (OFB) and the French Ministry of Ecological Transition (MTECT). The  
669 authors would like to thank all the members of the Explore2 consortium who contributed to  
670 the creation of this unique dataset for France.

671

672 **Financial support**

673

674 This research has been supported by the Office Français de la Biodiversité (Explore2  
675 project), the Ministère de la Transition écologique et Solidaire (Explore2 project)

676

677

678

679

680



681 **References**

682

683 Abbenante, S. E., Althoff, I., and Valdes-Abellan, J.: Comparative analysis of lumped and  
684 semi-distributed hydrological models in humid Mediterranean environments, *Hydrological*  
685 *Sciences Journal*, 69, 2481–2496, <https://doi.org/10.1080/02626667.2024.2413422>, 2024.

686 Alfieri, L., Burek, P., Feyen, L., and Forzieri, G.: Global warming increases the frequency of  
687 river floods in Europe, *Hydrol. Earth Syst. Sci.*, 19, 2247–2260, [https://doi.org/10.5194/hess-](https://doi.org/10.5194/hess-19-2247-2015)  
688 19-2247-2015, 2015.

689 Bathelemy, R., Brigode, P., Andréassian, V., Perrin, C., Moron, V., Gaucherel, C., Tric, E.,  
690 and Boisson, D.: Simbi: historical hydro-meteorological time series and signatures for 24  
691 catchments in Haiti, *Earth Syst. Sci. Data*, 16, 2073–2098, [https://doi.org/10.5194/essd-16-](https://doi.org/10.5194/essd-16-2073-2024)  
692 2073-2024, 2024.

693 Berghuijs, W. R., Woods, R. A., Hutton, C. J., and Sivapalan, M.: Dominant flood generating  
694 mechanisms across the United States: Flood Mechanisms Across the U.S., *Geophys. Res.*  
695 *Lett.*, 43, 4382–4390, <https://doi.org/10.1002/2016GL068070>, 2016.

696 Berghuijs, W. R., Harrigan, S., Molnar, P., Slater, L. J., and Kirchner, J. W.: The Relative  
697 Importance of Different Flood-Generating Mechanisms Across Europe, *Water Resour. Res.*,  
698 2019WR024841, <https://doi.org/10.1029/2019WR024841>, 2019.

699 Blöschl, G.: Flood generation: process patterns from the raindrop to the ocean, *Hydrol. Earth*  
700 *Syst. Sci.*, 26, 2469–2480, <https://doi.org/10.5194/hess-26-2469-2022>, 2022a.

701 Blöschl, G.: Three hypotheses on changing river flood hazards, *Hydrol. Earth Syst. Sci.*, 26,  
702 5015–5033, <https://doi.org/10.5194/hess-26-5015-2022>, 2022b.

703 Blöschl, G., Hall, J., Viglione, A., Perdigão, R. A. P., Parajka, J., Merz, B., Lun, D., Arheimer,  
704 B., Aronica, G. T., Bilibashi, A., Boháč, M., Bonacci, O., Borga, M., Čanjevac, I., Castellarin,  
705 A., Chirico, G. B., Claps, P., Frolova, N., Ganora, D., Gorbachova, L., Gül, A., Hannaford, J.,  
706 Harrigan, S., Kireeva, M., Kiss, A., Kjeldsen, T. R., Kohnová, S., Koskela, J. J., Ledvinka, O.,  
707 Macdonald, N., Mavrova-Guirguinova, M., Mediero, L., Merz, R., Molnar, P., Montanari, A.,  
708 Murphy, C., Osuch, M., Ovcharuk, V., Radevski, I., Salinas, J. L., Sauquet, E., Šraj, M.,  
709 Szolgay, J., Volpi, E., Wilson, D., Zaimi, K., and Živković, N.: Changing climate both  
710 increases and decreases European river floods, *Nature*, 573, 108–111,  
711 <https://doi.org/10.1038/s41586-019-1495-6>, 2019.

712 Blöschl, G., Kiss, A., Viglione, A., Barriendos, M., Böhm, O., Brázdil, R., Coeur, D.,  
713 Demarée, G., Llasat, M. C., Macdonald, N., Retsö, D., Roald, L., Schmocker-Fackel, P.,  
714 Amorim, I., Bělíková, M., Benito, G., Bertolin, C., Camuffo, D., Cornel, D., Doktor, R.,  
715 Elleder, L., Enzi, S., Garcia, J. C., Glaser, R., Hall, J., Haslinger, K., Hofstätter, M., Komma,  
716 J., Limanówka, D., Lun, D., Panin, A., Parajka, J., Petrić, H., Rodrigo, F. S., Rohr, C.,  
717 Schönbein, J., Schulte, L., Silva, L. P., Toonen, W. H. J., Valent, P., Waser, J., and Wetter,  
718 O.: Current European flood-rich period exceptional compared with past 500 years, *Nature*,  
719 583, 560–566, <https://doi.org/10.1038/s41586-020-2478-3>, 2020.

720 Brigode, P., Oudin, L., and Perrin, C.: Hydrological model parameter instability: A source of  
721 additional uncertainty in estimating the hydrological impacts of climate change?, *Journal of*  
722 *Hydrology*, 476, 410–425, <https://doi.org/10.1016/j.jhydrol.2012.11.012>, 2013.

723 Brunner, M. I., Swain, D. L., Wood, R. R., Willkofer, F., Done, J. M., Gilleland, E., and  
724 Ludwig, R.: An extremeness threshold determines the regional response of floods to  
725 changes in rainfall extremes, *Commun Earth Environ*, 2, 173,



- 726 <https://doi.org/10.1038/s43247-021-00248-x>, 2021.
- 727 Chauveau, M., Chazot, S., Perrin, C., Bourgin, P.-Y., Sauquet, E., Vidal, J.-P., Rouchy, N.,  
728 Martin, E., David, J., Norotte, T., Maugis, P., and De Lacaze, X.: Quels impacts des  
729 changements climatiques sur les eaux de surface en France à l'horizon 2070 ?, *La Houille*  
730 *Blanche*, 99, 5–15, <https://doi.org/10.1051/lhb/2013027>, 2013.
- 731 Clark, M. P., Wilby, R. L., Gutmann, E. D., Vano, J. A., Gangopadhyay, S., Wood, A. W.,  
732 Fowler, H. J., Prudhomme, C., Arnold, J. R., and Brekke, L. D.: Characterizing Uncertainty of  
733 the Hydrologic Impacts of Climate Change, *Curr Clim Change Rep*, 2, 55–64,  
734 <https://doi.org/10.1007/s40641-016-0034-x>, 2016.
- 735 Coppola, E., Nogherotto, R., Ciarlo', J. M., Giorgi, F., Van Meijgaard, E., Kadyrov, N., Iles,  
736 C., Corre, L., Sandstad, M., Somot, S., Nabat, P., Vautard, R., Levvasseur, G.,  
737 Schwingshackl, C., Sillmann, J., Kjellström, E., Nikulin, G., Aalbers, E., Lenderink, G.,  
738 Christensen, O. B., Boberg, F., Sørland, S. L., Demory, M., Bülow, K., Teichmann, C.,  
739 Warrach-Sagi, K., and Wulfmeyer, V.: Assessment of the European Climate Projections as  
740 Simulated by the Large EURO-CORDEX Regional and Global Climate Model Ensemble,  
741 *JGR Atmospheres*, 126, e2019JD032356, <https://doi.org/10.1029/2019JD032356>, 2021.
- 742 Cornelissen, T., Diekkrüger, B., and Giertz, S.: A comparison of hydrological models for  
743 assessing the impact of land use and climate change on discharge in a tropical catchment,  
744 *Journal of Hydrology*, 498, 221–236, <https://doi.org/10.1016/j.jhydrol.2013.06.016>, 2013.
- 745 Coron, L., Thirel, G., Delaigue, O., Perrin, C., and Andréassian, V.: The suite of lumped GR  
746 hydrological models in an R package, *Environmental Modelling & Software*, 94, 166–171,  
747 <https://doi.org/10.1016/j.envsoft.2017.05.002>, 2017.
- 748 Corre, L., Ribes, A., Bernus, S., Drouin, A., Morin, S., and Soubeyroux, J.-M.: Using regional  
749 warming levels to describe future climate change for services and adaptation: Application to  
750 the French reference trajectory for adaptation, *Climate Services*, 38, 100553,  
751 <https://doi.org/10.1016/j.cliser.2025.100553>, 2025.
- 752 Dakhlaoui, H., Ruelland, D., Trambay, Y., and Bargaoui, Z.: Evaluating the robustness of  
753 conceptual rainfall-runoff models under climate variability in northern Tunisia, *Journal of*  
754 *Hydrology*, 550, 201–217, <https://doi.org/10.1016/j.jhydrol.2017.04.032>, 2017.
- 755 De Lavenne, A., Andréassian, V., Thirel, G., Ramos, M. -H., and Perrin, C.: A Regularization  
756 Approach to Improve the Sequential Calibration of a Semidistributed Hydrological Model,  
757 *Water Resources Research*, 55, 8821–8839, <https://doi.org/10.1029/2018WR024266>, 2019.
- 758 Di Sante, F., Coppola, E., and Giorgi, F.: Projections of river floods in Europe using EURO-  
759 CORDEX, CMIP5 and CMIP6 simulations, *Int J Climatol*, 41, 3203–3221,  
760 <https://doi.org/10.1002/joc.7014>, 2021.
- 761 Do, H. X., Zhao, F., Westra, S., Leonard, M., Gudmundsson, L., Boulange, J. E. S., Chang,  
762 J., Ciais, P., Gerten, D., Gosling, S. N., Müller Schmied, H., Stacke, T., Telteu, C.-E., and  
763 Wada, Y.: Historical and future changes in global flood magnitude – evidence from a model-  
764 observation investigation, *Hydrol. Earth Syst. Sci.*, 24, 1543–1564,  
765 <https://doi.org/10.5194/hess-24-1543-2020>, 2020.
- 766 Dorchie, D.: hubeau: an R package for the Hub'Eau APIs,  
767 <https://doi.org/10.57745/XKN6NC>, 2022.
- 768 Efron, B.: Bootstrap Methods: Another Look at the Jackknife, *Ann. Statist.*, 7,



- 769 <https://doi.org/10.1214/aos/1176344552>, 1979.
- 770 Fabre, J., Ruelland, D., Dezetter, A., and Grouillet, B.: Sustainability of water uses in  
771 managed hydrosystems: human-and climate-induced changes for the mid-21st century,  
772 *Hydrol. Earth Syst. Sci.*, 20, 3129–3147, <https://doi.org/10.5194/hess-20-3129-2016>, 2016.
- 773 Froidevaux, P., Schwanbeck, J., Weingartner, R., Chevalier, C., and Martius, O.: Flood  
774 triggering in Switzerland: the role of daily to monthly preceding precipitation, *Hydrol. Earth*  
775 *Syst. Sci.*, 19, 3903–3924, <https://doi.org/10.5194/hess-19-3903-2015>, 2015.
- 776 Givati, A., Thirel, G., Rosenfeld, D., and Paz, D.: Climate change impacts on streamflow at  
777 the upper Jordan River based on an ensemble of regional climate models, *Journal of*  
778 *Hydrology: Regional Studies*, 21, 92–109, <https://doi.org/10.1016/j.ejrh.2018.12.004>, 2019.
- 779 Grill, G., Lehner, B., Thieme, M., Geenen, B., Tickner, D., Antonelli, F., Babu, S., Borrelli, P.,  
780 Cheng, L., Crochetiere, H., Ehalt Macedo, H., Filgueiras, R., Goichot, M., Higgins, J., Hogan,  
781 Z., Lip, B., McClain, M. E., Meng, J., Mulligan, M., Nilsson, C., Olden, J. D., Opperman, J. J.,  
782 Petry, P., Reidy Liermann, C., Sáenz, L., Salinas-Rodríguez, S., Schelle, P., Schmitt, R. J.,  
783 P., Snider, J., Tan, F., Tockner, K., Valdujo, P. H., van Soesbergen, A., and Zarfl, C.:  
784 Mapping the world's free-flowing rivers, *Nature*, 569, 215–221,  
785 <https://doi.org/10.1038/s41586-019-1111-9>, 2019.
- 786 Gupta, H. V., Kling, H., Yilmaz, K. K., and Martinez, G. F.: Decomposition of the mean  
787 squared error and NSE performance criteria: Implications for improving hydrological  
788 modelling, *Journal of Hydrology*, 377, 80–91, <https://doi.org/10.1016/j.jhydrol.2009.08.003>,  
789 2009.
- 790 Hamed, K. H. and Ramachandra Rao, A.: A modified Mann-Kendall trend test for  
791 autocorrelated data, *Journal of Hydrology*, 204, 182–196, [https://doi.org/10.1016/S0022-1694\(97\)00125-X](https://doi.org/10.1016/S0022-1694(97)00125-X), 1998.
- 793 Ho, M., Nathan, R., Wasko, C., Vogel, E., and Sharma, A.: Projecting changes in flood event  
794 runoff coefficients under climate change, *Journal of Hydrology*, 615, 128689,  
795 <https://doi.org/10.1016/j.jhydrol.2022.128689>, 2022.
- 796 Hodgkins, G. A., Whitfield, P. H., Burn, D. H., Hannaford, J., Renard, B., Stahl, K., Fleig, A.  
797 K., Madsen, H., Mediero, L., Korhonen, J., Murphy, C., and Wilson, D.: Climate-driven  
798 variability in the occurrence of major floods across North America and Europe, *Journal of*  
799 *Hydrology*, 552, 704–717, <https://doi.org/10.1016/j.jhydrol.2017.07.027>, 2017.
- 800 Hrachowitz, M. and Clark, M. P.: HESS Opinions: The complementary merits of competing  
801 modelling philosophies in hydrology, *Hydrol. Earth Syst. Sci.*, 21, 3953–3973,  
802 <https://doi.org/10.5194/hess-21-3953-2017>, 2017.
- 803 Intergovernmental Panel On Climate Change (ipcc): Climate Change 2021 – The Physical  
804 Science Basis: Working Group I Contribution to the Sixth Assessment Report of the  
805 Intergovernmental Panel on Climate Change, 1st ed., Cambridge University Press,  
806 <https://doi.org/10.1017/9781009157896>, 2023.
- 807 Ivancic, T. J. and Shaw, S. B.: Examining why trends in very heavy precipitation should not  
808 be mistaken for trends in very high river discharge, *Climatic Change*, 133, 681–693,  
809 <https://doi.org/10.1007/s10584-015-1476-1>, 2015.
- 810 Jacob, D., Kotova, L., Teichmann, C., Sobolowski, S. P., Vautard, R., Donnelly, C.,  
811 Koutroulis, A. G., Grillakis, M. G., Tsanis, I. K., Damm, A., Sakalli, A., and van Vliet, M. T. H.:





- 812 Climate Impacts in Europe Under +1.5°C Global Warming, *Earth's Future*, 6, 264–285,  
813 <https://doi.org/10.1002/2017EF000710>, 2018.
- 814 Jahanshahi, A., Booij, M. J., and Patil, S. D.: Dependence of rainfall–runoff model  
815 performance on calibration conditions under changing climatic conditions, *Hydrological  
816 Sciences Journal*, 1–16, <https://doi.org/10.1080/02626667.2024.2441325>, 2025.
- 817 Jiang, S., Bevacqua, E., and Zscheischler, J.: River flooding mechanisms and their changes  
818 in Europe revealed by explainable machine learning, *Hydrol. Earth Syst. Sci.*, 26, 6339–  
819 6359, <https://doi.org/10.5194/hess-26-6339-2022>, 2022.
- 820 Kay, A.: Differences in hydrological impacts using regional climate model and nested  
821 convection-permitting model data, *Climatic Change*, 173, 11, [https://doi.org/10.1007/s10584-  
822 022-03405-z](https://doi.org/10.1007/s10584-022-03405-z), 2022.
- 823 Kemter, M., Merz, B., Marwan, N., Vorogushyn, S., and Blöschl, G.: Joint Trends in Flood  
824 Magnitudes and Spatial Extents Across Europe, *Geophys. Res. Lett.*, 47,  
825 <https://doi.org/10.1029/2020GL087464>, 2020.
- 826 Kemter, M., Marwan, N., Villarini, G., and Merz, B.: Controls on Flood Trends Across the  
827 United States, *Water Resources Research*, 59, e2021WR031673,  
828 <https://doi.org/10.1029/2021WR031673>, 2023.
- 829 Killick, R., Fearnhead, P., and Eckley, I. A.: Optimal Detection of Changepoints With a Linear  
830 Computational Cost, *Journal of the American Statistical Association*, 107, 1590–1598,  
831 <https://doi.org/10.1080/01621459.2012.737745>, 2012.
- 832 Kim, J., Johnson, L., Cifelli, R., Thorstensen, A., and Chandrasekar, V.: Assessment of  
833 antecedent moisture condition on flood frequency: An experimental study in Napa River  
834 Basin, CA, *Journal of Hydrology: Regional Studies*, 26, 100629,  
835 <https://doi.org/10.1016/j.ejrh.2019.100629>, 2019.
- 836 Klemesš, V.: Operational testing of hydrological simulation models, *Hydrological Sciences  
837 Journal*, 31, 13–24, <https://doi.org/10.1080/02626668609491024>, 1986.
- 838 Knutti, R. and Sedláček, J.: Robustness and uncertainties in the new CMIP5 climate model  
839 projections, *Nature Clim Change*, 3, 369–373, <https://doi.org/10.1038/nclimate1716>, 2013.
- 840 Koenker, R. and Bassett, G.: Regression Quantiles, *Econometrica*, 46, 33,  
841 <https://doi.org/10.2307/1913643>, 1978.
- 842 Kuana, L. A., Almeida, A. S., Mercuri, E. G. F., and Noe, S. M.: Regionalization of GR4J  
843 model parameters for river flow prediction in Paraná, Brazil, *Hydrol. Earth Syst. Sci.*, 28,  
844 3367–3390, <https://doi.org/10.5194/hess-28-3367-2024>, 2024.
- 845 Lemaitre-Basset, T., Collet, L., Thirel, G., Parajka, J., Evin, G., and Hingray, B.: Climate  
846 change impact and uncertainty analysis on hydrological extremes in a French Mediterranean  
847 catchment, *Hydrological Sciences Journal*, 66, 888–903,  
848 <https://doi.org/10.1080/02626667.2021.1895437>, 2021.
- 849 Lemaitre-Basset, T., Thirel, G., Oudin, L., and Dorchies, D.: Water use scenarios versus  
850 climate change: Investigating future water management of the French part of the Moselle,  
851 *Journal of Hydrology: Regional Studies*, 54, 101855,  
852 <https://doi.org/10.1016/j.ejrh.2024.101855>, 2024.



- 853 Lucas-Picher, P., Argüeso, D., Brisson, E., Trambly, Y., Berg, P., Lemonsu, A., Kotlarski,  
854 S., and Caillaud, C.: CONVECTION -permitting modeling with regional climate models: Latest  
855 developments and next steps, *WIREs Climate Change*, 12, e731,  
856 <https://doi.org/10.1002/wcc.731>, 2021.
- 857 Lun, D., Fischer, S., Viglione, A., and Blöschl, G.: Detecting Flood-Rich and Flood-Poor  
858 Periods in Annual Peak Discharges Across Europe, *Water Resources Research*, 56,  
859 e2019WR026575, <https://doi.org/10.1029/2019WR026575>, 2020.
- 860 Lyne, V. D. and Hollick, M.: Stochastic time-variable rainfall runoff modelling, *Hydrology and*  
861 *Water Resources Symposium*, Institution of Engineers, Australia, Perth (1979), Barton,  
862 Australia, 1979.
- 863 Maraun, D., Shepherd, T. G., Widmann, M., Zappa, G., Walton, D., Gutiérrez, J. M.,  
864 Hagemann, S., Richter, I., Soares, P. M. M., Hall, A., and Mearns, L. O.: Towards process-  
865 informed bias correction of climate change simulations, *Nature Clim Change*, 7, 764–773,  
866 <https://doi.org/10.1038/nclimate3418>, 2017.
- 867 Marson, P., Corre, L., Soubeyroux, J.-M., Sauquet, É., and Explore2: Rapport de synthèse  
868 sur les projections climatiques régionalisées, <https://doi.org/10.57745/PUR7ML>, 2024.
- 869 McMillan, H., Araki, R., Bolotin, L., Kim, D.-H., Coxon, G., Clark, M., and Seibert, J.: Global  
870 patterns in observed hydrologic processes, *Nat Water*, [https://doi.org/10.1038/s44221-025-](https://doi.org/10.1038/s44221-025-00407-w)  
871 [00407-w](https://doi.org/10.1038/s44221-025-00407-w), 2025.
- 872 Meinshausen, M., Nicholls, Z. R. J., Lewis, J., Gidden, M. J., Vogel, E., Freund, M., Beyerle,  
873 U., Gessner, C., Nauels, A., Bauer, N., Canadell, J. G., Daniel, J. S., John, A., Krummel, P.  
874 B., Luderer, G., Meinshausen, N., Montzka, S. A., Rayner, P. J., Reimann, S., Smith, S. J.,  
875 Van Den Berg, M., Velders, G. J. M., Vollmer, M. K., and Wang, R. H. J.: The shared socio-  
876 economic pathway (SSP) greenhouse gas concentrations and their extensions to 2500,  
877 *Geosci. Model Dev.*, 13, 3571–3605, <https://doi.org/10.5194/gmd-13-3571-2020>, 2020.
- 878 Nepal, S., Chen, J., Penton, D. J., Neumann, L. E., Zheng, H., and Wahid, S.: Spatial GR4J  
879 conceptualization of the Tamor glaciated alpine catchment in Eastern Nepal: evaluation of  
880 GR4JSG against streamflow and MODIS snow extent, *Hydrological Processes*, 31, 51–68,  
881 <https://doi.org/10.1002/hyp.10962>, 2017.
- 882 Perrin, C., Michel, C., and Andréassian, V.: Improvement of a parsimonious model for  
883 streamflow simulation, *Journal of Hydrology*, 279, 275–289, [https://doi.org/10.1016/S0022-](https://doi.org/10.1016/S0022-1694(03)00225-7)  
884 [1694\(03\)00225-7](https://doi.org/10.1016/S0022-1694(03)00225-7), 2003.
- 885 Poncet, N., Lucas-Picher, P., Trambly, Y., Thirel, G., Vergara, H., Gourley, J., and Alias, A.:  
886 Does a convection-permitting regional climate model bring new perspectives on the  
887 projection of Mediterranean floods?, *Nat. Hazards Earth Syst. Sci.*, 24, 1163–1183,  
888 <https://doi.org/10.5194/nhess-24-1163-2024>, 2024.
- 889 Rogger, M., Agnoletti, M., Alaoui, A., Bathurst, J. C., Bodner, G., Borga, M., Chaplot, V.,  
890 Gallart, F., Glatzel, G., Hall, J., Holden, J., Holko, L., Horn, R., Kiss, A., Kohnová, S.,  
891 Leitingner, G., Lennartz, B., Parajka, J., Perdigão, R., Peth, S., Plavcová, L., Quinton, J. N.,  
892 Robinson, M., Salinas, J. L., Santoro, A., Szolgay, J., Tron, S., van den Akker, J. J. H.,  
893 Viglione, A., and Blöschl, G.: Land use change impacts on floods at the catchment scale:  
894 Challenges and opportunities for future research: LAND USE CHANGE IMPACTS ON  
895 FLOODS, *Water Resour. Res.*, 53, 5209–5219, <https://doi.org/10.1002/2017WR020723>,  
896 2017.



- 897 Roudier, P., Andersson, J. C. M., Donnelly, C., Feyen, L., Greuell, W., and Ludwig, F.:  
898 Projections of future floods and hydrological droughts in Europe under a +2°C global  
899 warming, *Climatic Change*, 135, 341–355, <https://doi.org/10.1007/s10584-015-1570-4>, 2016.
- 900 Santos, L., Andréassian, V., Sonnenborg, T. O., Lindström, G., De Lavenne, A., Perrin, C.,  
901 Collet, L., and Thirel, G.: Lack of robustness of hydrological models: a large-sample  
902 diagnosis and an attempt to identify hydrological and climatic drivers, *Hydrol. Earth Syst.*  
903 *Sci.*, 29, 683–700, <https://doi.org/10.5194/hess-29-683-2025>, 2025.
- 904 Sauquet, É., Héraud, L., Bonneau, J., Reverdy, A., Strohmenger, L., Vidal, J.-P., and  
905 Explore2: Diagnostic des modèles hydrologiques : Des données aux résultats,  
906 <https://doi.org/10.57745/S6PQXD>, 2024.
- 907 Sauquet E., Evin G., Siauue S., Aissat R., Arnaud P., Berel M., Bonneau J., Branger F.,  
908 Caballero Y., Colleoni F., Ducharne A., Gailhard J., Habets F., Hendrickx F., Héraud L.,  
909 Hingray B., Huang P., Jaouen T., Jeantet A., Lanini S., Le Lay M., Magand C., Mimeau L.,  
910 Monteil C., Munier S., Perrin C., Robelin O., Rousset F., Soubeyroux J.-M., Strohmenger L.,  
911 Thirel G., Tocquer F., Tramblay Y., Vergnes J.-P., Vidal J.-P., A large transient multi-  
912 scenario multi-model ensemble of future streamflows and groundwater projections in France,  
913 *Hydrology and Earth System Sciences*, submitted, 2025.
- 914 Scussolini, P., Luu, L. N., Philip, S., Berghuijs, W. R., Eilander, D., Aerts, J. C. J. H., Kew, S.  
915 F., Van Oldenborgh, G. J., Toonen, W. H. J., Volkholz, J., and Coumou, D.: Challenges in  
916 the attribution of river flood events, *WIREs Climate Change*, e874,  
917 <https://doi.org/10.1002/wcc.874>, 2023.
- 918 Sen, P. K.: Estimates of the Regression Coefficient Based on Kendall's Tau, *Journal of the*  
919 *American Statistical Association*, 63, 1379–1389,  
920 <https://doi.org/10.1080/01621459.1968.10480934>, 1968.
- 921 Sharma, A., Wasko, C., and Lettenmaier, D. P.: If Precipitation Extremes Are Increasing,  
922 Why Aren't Floods?, *Water Resour. Res.*, 54, 8545–8551,  
923 <https://doi.org/10.1029/2018WR023749>, 2018.
- 924 Stein, L., Pianosi, F., and Woods, R.: Event-based classification for global study of river  
925 flood generating processes, *Hydrological Processes*, 34, 1514–1529,  
926 <https://doi.org/10.1002/hyp.13678>, 2020.
- 927 Stein, L., Clark, M. P., Knoben, W. J. M., Pianosi, F., and Woods, R. A.: How Do Climate  
928 and Catchment Attributes Influence Flood Generating Processes? A Large-Sample Study for  
929 671 Catchments Across the Contiguous USA, *Water Res.*, 57,  
930 <https://doi.org/10.1029/2020WR028300>, 2021.
- 931 Stephens, C. M., Johnson, F. M., and Marshall, L. A.: Implications of future climate change  
932 for event-based hydrologic models, *Advances in Water Resources*, 119, 95–110,  
933 <https://doi.org/10.1016/j.advwatres.2018.07.004>, 2018.
- 934 Stephens, C. M., Marshall, L. A., and Johnson, F. M.: Investigating strategies to improve  
935 hydrologic model performance in a changing climate, *Journal of Hydrology*, 579, 124219,  
936 <https://doi.org/10.1016/j.jhydrol.2019.124219>, 2019.
- 937 Strohmenger, L., Sauquet, E., Bernard, C., Bonneau, J., Branger, F., Bresson, A., Brigode,  
938 P., Buzier, R., Delaigue, O., Devers, A., Evin, G., Fournier, M., Hsu, S.-C., Lanini, S., De  
939 Lavenne, A., Lemaitre-Basset, T., Magand, C., Mendoza Guimarães, G., Mentha, M.,  
940 Munier, S., Perrin, C., Podechard, T., Rouchy, L., Sadki, M., Soutif-Bellenger, M., Tilmant,



- 941 F., Trambly, Y., Véron, A.-L., Vidal, J.-P., and Thirel, G.: On the visual detection of non-  
942 natural records in streamflow time series: challenges and impacts, *Hydrol. Earth Syst. Sci.*,  
943 27, 3375–3391, <https://doi.org/10.5194/hess-27-3375-2023>, 2023.
- 944 Strohmer, L., Collet, L., Andréassian, V., Corre, L., Rousset, F., and Thirel, G.: Köppen–  
945 Geiger climate classification across France based on an ensemble of high-resolution climate  
946 projections, *Comptes Rendus. Géoscience*, 356, 67–82, <https://doi.org/10.5802/crgeos.263>,  
947 2024.
- 948 Tarasova, L., Basso, S., Zink, M., and Merz, R.: Exploring Controls on Rainfall-Runoff  
949 Events: 1. Time Series-Based Event Separation and Temporal Dynamics of Event Runoff  
950 Response in Germany, *Water Resour. Res.*, 54, 7711–7732,  
951 <https://doi.org/10.1029/2018WR022587>, 2018.
- 952 Tarasova, L., Merz, R., Kiss, A., Basso, S., Blöschl, G., Merz, B., Viglione, A., Plötner, S.,  
953 Guse, B., Schumann, A., Fischer, S., Ahrens, B., Anwar, F., Bárdossy, A., Bühler, P.,  
954 Haberlandt, U., Kreibich, H., Krug, A., Lun, D., Müller-Thomy, H., Pidoto, R., Primo, C.,  
955 Seidel, J., Vorogushyn, S., and Wietzke, L.: Causative classification of river flood events,  
956 *WIREs Water*, 6, <https://doi.org/10.1002/wat2.1353>, 2019.
- 957 Tarasova, L., Basso, S., Wendi, D., Viglione, A., Kumar, R., and Merz, R.: A Process-Based  
958 Framework to Characterize and Classify Runoff Events: The Event Typology of Germany,  
959 *Water Resour. Res.*, 56, <https://doi.org/10.1029/2019WR026951>, 2020.
- 960 Tarasova, L., Lun, D., Merz, R., Blöschl, G., Basso, S., Bertola, M., Miniussi, A., Rakovec,  
961 O., Samaniego, L., Thober, S., and Kumar, R.: Shifts in flood generation processes  
962 exacerbate regional flood anomalies in Europe, *Commun Earth Environ*, 4, 49,  
963 <https://doi.org/10.1038/s43247-023-00714-8>, 2023.
- 964 Tarek, M., Brissette, F., and Arsenault, R.: Uncertainty of gridded precipitation and  
965 temperature reference datasets in climate change impact studies, *Hydrol. Earth Syst. Sci.*,  
966 25, 3331–3350, <https://doi.org/10.5194/hess-25-3331-2021>, 2021.
- 967 Taylor, K. E., Stouffer, R. J., and Meehl, G. A.: An Overview of CMIP5 and the Experiment  
968 Design, *Bulletin of the American Meteorological Society*, 93, 485–498,  
969 <https://doi.org/10.1175/BAMS-D-11-00094.1>, 2012.
- 970 Terray, L. and Boé, J.: Quantifying 21st-century France climate change and related  
971 uncertainties, *Comptes Rendus. Géoscience*, 345, 136–149,  
972 <https://doi.org/10.1016/j.crte.2013.02.003>, 2013.
- 973 Teutschbein, C. and Seibert, J.: Bias correction of regional climate model simulations for  
974 hydrological climate-change impact studies: Review and evaluation of different methods,  
975 *Journal of Hydrology*, 456–457, 12–29, <https://doi.org/10.1016/j.jhydrol.2012.05.052>, 2012.
- 976 Thirel, G., Andréassian, V., Perrin, C., Audouy, J.-N., Berthet, L., Edwards, P., Folton, N.,  
977 Furusho, C., Kuertz, A., Lerat, J., Lindström, G., Martin, E., Mathevet, T., Merz, R., Parajka,  
978 J., Ruelland, D., and Vaze, J.: Hydrology under change: an evaluation protocol to investigate  
979 how hydrological models deal with changing catchments, *Hydrological Sciences Journal*, 60,  
980 1184–1199, <https://doi.org/10.1080/02626667.2014.967248>, 2015a.
- 981 Thirel, G., Andréassian, V., and Perrin, C.: On the need to test hydrological models under  
982 changing conditions, *Hydrological Sciences Journal*, 60, 1165–1173,  
983 <https://doi.org/10.1080/02626667.2015.1050027>, 2015b.



- 984 Thirel, G., Gerlinger, K., Perrin, C., Drogue, G., Renard, B., and Wagner, J.-P.: Quels futurs  
985 possibles pour les débits des affluents français du Rhin (Moselle, Sarre, Ill) ?, *La Houille*  
986 *Blanche*, 105, 140–149, <https://doi.org/10.1051/lhb/2019039>, 2019.
- 987 Tian, Y., Xu, Y.-P., and Zhang, X.-J.: Assessment of Climate Change Impacts on River High  
988 Flows through Comparative Use of GR4J, HBV and Xinanjiang Models, *Water Resour*  
989 *Manage*, 27, 2871–2888, <https://doi.org/10.1007/s11269-013-0321-4>, 2013.
- 990 Tramblay, Y. and Somot, S.: Future evolution of extreme precipitation in the Mediterranean,  
991 *Climatic Change*, 151, 289–302, <https://doi.org/10.1007/s10584-018-2300-5>, 2018.
- 992 Tramblay, Y., Mimeau, L., Neppel, L., Vinet, F., and Sauquet, E.: Detection and attribution of  
993 flood trends in Mediterranean basins, *Hydrol. Earth Syst. Sci.*, 23, 4419–4431,  
994 <https://doi.org/10.5194/hess-23-4419-2019>, 2019.
- 995 Tramblay, Y., Villarini, G., Khalki, E. M., Gründemann, G., and Hughes, D.: Evaluation of the  
996 Drivers Responsible for Flooding in Africa, *Water Resources Research*, 57,  
997 <https://doi.org/10.1029/2021WR029595>, 2021.
- 998 Tramblay, Y., Villarini, G., Saidi, M. E., Massari, C., and Stein, L.: Classification of flood-  
999 generating processes in Africa, *Sci Rep*, 12, 18920, [https://doi.org/10.1038/s41598-022-](https://doi.org/10.1038/s41598-022-23725-5)  
1000 23725-5, 2022.
- 1001 Tramblay, Y., Arnaud, P., Artigue, G., Lang, M., Paquet, E., Neppel, L., and Sauquet, E.:  
1002 Changes in Mediterranean flood processes and seasonality, *Hydrol. Earth Syst. Sci.*, 27,  
1003 2973–2987, <https://doi.org/10.5194/hess-27-2973-2023>, 2023.
- 1004 Tramblay, Y., Sauquet, É., Arnaud, P., Rousset, F., Soubeyroux, J.-M., Hingray, B., Jaouen,  
1005 T., Jeantet, A., Munier, S., Vergnes, J.-P., and Explore2: Scénarios d'extrêmes  
1006 hydrologiques, <https://doi.org/10.57745/2XDJ5H>, 2024.
- 1007 Valéry, A., Andréassian, V., and Perrin, C.: 'As simple as possible but not simpler': What is  
1008 useful in a temperature-based snow-accounting routine? Part 2 – Sensitivity analysis of the  
1009 Cemaneige snow accounting routine on 380 catchments, *Journal of Hydrology*, 517, 1176–  
1010 1187, <https://doi.org/10.1016/j.jhydrol.2014.04.058>, 2014.
- 1011 Vautard, R., Kadyrov, N., Iles, C., Boberg, F., Buonomo, E., Bülow, K., Coppola, E., Corre,  
1012 L., Van Meijgaard, E., Nogherotto, R., Sandstad, M., Schwingshackl, C., Somot, S., Aalbers,  
1013 E., Christensen, O. B., Ciarlo, J. M., Demory, M., Giorgi, F., Jacob, D., Jones, R. G., Keuler,  
1014 K., Kjellström, E., Lenderink, G., Levavasseur, G., Nikulin, G., Sillmann, J., Solidoro, C.,  
1015 Sørland, S. L., Steger, C., Teichmann, C., Warrach-Sagi, K., and Wulfmeyer, V.: Evaluation  
1016 of the Large EURO-CORDEX Regional Climate Model Ensemble, *JGR Atmospheres*, 126,  
1017 e2019JD032344, <https://doi.org/10.1029/2019JD032344>, 2021.
- 1018 Verfaillie, D., Déqué, M., Morin, S., and Lafaysse, M.: The method ADAMONT v1.0 for  
1019 statistical adjustment of climate projections applicable to energy balance land surface  
1020 models, *Geosci. Model Dev.*, 10, 4257–4283, <https://doi.org/10.5194/gmd-10-4257-2017>,  
1021 2017.
- 1022 Vidal, J., Martin, E., Franchistéguy, L., Baillon, M., and Soubeyroux, J.: A 50-year high-  
1023 resolution atmospheric reanalysis over France with the Safran system, *Intl Journal of*  
1024 *Climatology*, 30, 1627–1644, <https://doi.org/10.1002/joc.2003>, 2010.
- 1025 Vidal, J.-P., Hingray, B., Magand, C., Sauquet, E., and Ducharne, A.: Hierarchy of climate  
1026 and hydrological uncertainties in transient low-flow projections, *Hydrol. Earth Syst. Sci.*, 20,



- 1027 3651–3672, <https://doi.org/10.5194/hess-20-3651-2016>, 2016.
- 1028 Wasko, C. and Nathan, R.: Influence of changes in rainfall and soil moisture on trends in  
1029 flooding, *Journal of Hydrology*, 575, 432–441, <https://doi.org/10.1016/j.jhydrol.2019.05.054>,  
1030 2019.
- 1031 Wasko, C., Guo, D., Ho, M., Nathan, R., and Vogel, E.: Diverging projections for flood and  
1032 rainfall frequency curves, *Journal of Hydrology*, 620, 129403,  
1033 <https://doi.org/10.1016/j.jhydrol.2023.129403>, 2023.
- 1034 Yang, L., Yang, Y., Villarini, G., Li, X., Hu, H., Wang, L., Blöschl, G., and Tian, F.: Climate  
1035 More Important for Chinese Flood Changes Than Reservoirs and Land Use, *Geophys Res*  
1036 *Lett*, 48, <https://doi.org/10.1029/2021GL093061>, 2021.
- 1037 Zahar, Y., Ghorbel, A., and Albergel, J.: Impacts of large dams on downstream flow  
1038 conditions of rivers: Aggradation and reduction of the Medjerda channel capacity  
1039 downstream of the Sidi Salem dam (Tunisia), *Journal of Hydrology*, 351, 318–330,  
1040 <https://doi.org/10.1016/j.jhydrol.2007.12.019>, 2008.
- 1041 Zhang, S., Zhou, L., Zhang, L., Yang, Y., Wei, Z., Zhou, S., Yang, D., Yang, X., Wu, X.,  
1042 Zhang, Y., Li, X., and Dai, Y.: Reconciling disagreement on global river flood changes in a  
1043 warming climate, *Nat. Clim. Chang.*, 12, 1160–1167, [https://doi.org/10.1038/s41558-022-](https://doi.org/10.1038/s41558-022-01539-7)  
1044 01539-7, 2022.
- 1045